AUT Journal of Modeling and Simulation

AUT J. Model. Simul., 51(2) (2019) 153-162
DOI: 10.22060/miscj.2019.15569.5136

Control of a 2-DoF robotic arm using a P300-based brain-computer interface

G. Garakani[1], H. Ghane[2,*], M.B. Menhaj[3]

[1] Department of Electrical Engineering, Tehran University, Tehran, Iran
[2] Department of Electrical Engineering, Islamic Azad University, Bandar Anzali, Iran
[3] Department of Electrical Engineering, Amirkabir University of Technology, Tehran, Iran

ABSTRACT: In this study, a novel control algorithm, based on a P300-based brain-computer interface (BCI) is deployed to control a 2-DoF robotic arm. Eight subjects, including five men and three women, perform a 2-dimensional target tracking in a simulated environment. Their EEG (Electroencephalography) signals from the visual cortex are recorded and P300 components are extracted and evaluated to deliver a real-time BCI-based controller. The volunteer's intention is recognized and will be decoded as an appropriate command to control the cursor. The final processed BCI output is used to control a simulated robotic arm in a 2-dimensional space. The results show that the system allows the robot's end-effector to move between arbitrary positions in a point-to-point session with the desired accuracy. This model is tested and compared on the Dataset II of the BCI competition. The best result is obtained with a multi-classifier solution with a recognition rate of 97 percent, without channel selection before the classification.

Review History:
Received: 2019-01-02
Revised: 2019-05-31
Accepted: 2019-06-08
Available Online: 2019-12-01

Keywords:
Brain-computer interface (BCI)
EEG
P300 Potential
Classification
2-DoF robotic arm

1. Introduction

"Pay attention" to something is an act that is frequently performed in daily life. This behavior occurs at the spontaneous electrical activity EEG by the appearance of a wave called P300. This wave was first reported in 1965 [1]. It appears as a positive deflection in the EEG signals approximately 250–500 *ms* following the presentation of a rare, deviant or target stimulus. P300 has been widely utilized in studies on brain activity disorders [2], [3], memory illusion and lie detection [4], [5], [6] and as the input of a BCI system [7]. In order to detect the P300 wave in noisy EEG signals, feature extraction methods combined with robust classifiers are generally used to extract hidden information from such signals and to classify them accurately. Utilizing electrical activity of neuron cortex ensemble to control a robotic arm was a winning goal that attracted researchers to study about BCI. Generally speaking, BCI makes a direct connection between man and an external tool [8]; however, for practical usages of this system, BCI can be defined as a system that establishes a connection between a man and his surrounding environment, which can be practiced through the brain [9].

Nowadays, the interface of brain and computer is a far-reaching topic; On the other hand, deleting this interface and installing a chip inside the human brain can be potentially harmful and only a few experiments have been done on the mice [10], [11], [12]. These systems can be used in various applications such as helping patients who are relatively mentally healthy but have moving troubles, like patients with Amyotrophic Lateral Sclerosis (ALS) and Spinal Cord Injury (SCI) or those with disorders that impair the movement of their organs in connection with the environment [13], [14]. Also, BCI systems can be used to simplify the connection of user with other objects and devices such as gaming consoles and smartphones [15].

Designing a proper BCI experiment that has high speed and accuracy in detecting P300 is vital. Visual test designs for P300 detection generally have two patterns; In the first pattern named as the oddball paradigm, there is a 6×6 matrix of English alphabet letters and numbers that each row and column of this matrix is switched on and off randomly. The signal is typically measured most strongly by the electrodes covering the parietal lobe. The presence, magnitude, topography and emergence time of this signal are often considered as metrics of cognitive function in decision-making processes. The detection of a P300 wave is equivalent to the detection of where the user had been looking 300 ms before its detection. In a P300 speller, the main goal is to detect the P300 peaks in the EEG, accurately and instantly. The accuracy of this detection will ensure a high information transfer rate between the user and the machine [8], [10].

The second pattern is used in applications such as choosing the desired direction, 2-D cursor control [17], [18], games [19], and general applications in which a user faces

*Corresponding author's email: hamed_ghane_s@aut.ac.ir

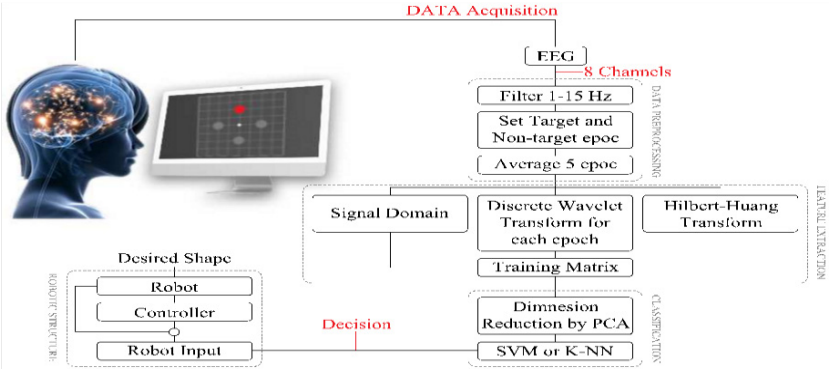

Fig. 1.: The procedure of controlling a robot by a BCI system.

some choices. In this pattern, There are some bulbs and each one indicates one choice and is randomly switched on and off in each round. The attention of the user to one of these bulbs makes P300 detectable in EEG. This pattern is applied in the paper and then the output of the BCI is used to actuate the end-effector of a simulated robotic arm.

Here, the EEG signals are used to control a simulated 2-degrees of freedom (DoF) robotic arm in a point-to-point real-time session. The robot comprises two revolute joints make it possible for the end-effector to move across a plane. The output of BCI is classified into four main decisions that make the robot to move in four main directions: up, down, left and right. The output of BCI is fed into a pre-processing unit and this unit reads the last brain decision and translates it into a reference position for the robotic arm. Eventually, the end-effector moves to follow user's directional orders.

The whole BCI task is performed in four steps, as shown in Fig. 1. The first step is to design a test associated with the final goal. The second one is to record the EEG signals, followed by a prompt and accurate detection of P300 waves. The third is to process the recorded data. Since brain signals are of low domains, the event-related potentials (ERPs) have a small signal to noise ratio (SNR); therefore, by applying a band-pass filter, almost all noises could be removed. Then through a Wavelet and Hilbert transforms, features are collected. In order to detect the subject command, the input data are classified utilizing K-nearest neighbors (KNN) and support vector machine (SVM) classifiers [24], [25], [26]. Finally, the fourth step is to establish a protocol in order to obtain an efficient connection between the brain and external tools.

The rest of the paper is organized as follows: Section 2 describes the recording data process and the primary key factors to improve the results. Section 3 focuses on preprocessing and filtering the recorded data. Section 4 discusses EEG signal feature extraction, and section 5 presents the classification algorithms. Section 6 proposes the robotic structure and control algorithm as the final application. Simulation results are illustrated in section 7. Finally, the conclusion is presented in Section 8.

2. Data Acquisition

In this section, the protocol for designing the task and performance of the recording device are introduced.

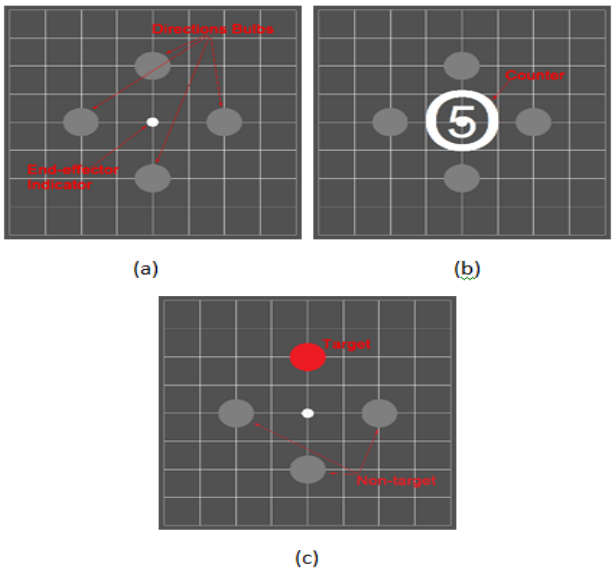

Fig. 2.: The designed GUI for controlling robotic arm (a) four bulbs as the four directions, (b) beginning the task with a counter, (c) target and non-target definition.

2-1- Task design

Task design is an essential part of every BCI experiment. More complicated tasks can result in more desirable outputs; however executing this complicated task can be very difficult in practice. Therefore, there should be a tradeoff between the simplicity of the task and accuracy of the outputs. In addition, factors such as age, gender, education, or every other feature which could potentially affect the results should be carefully considered. Besides, an isolated location, barren of any distraction and noise distortion, should be assigned for the task.

In this study, based on the information about the time of the task and distance of the bulbs given in the protocols of [27], [28], the primary task has been designed and has performed on subjects. Due to the possible downsides, some corrections like tuning the bulbs' distance have been applied after repeating the task several times. The task has carried out

on eight subjects (three women and five men) and the essential data for the research has been obtained. In order to achieve the best results, the primary test data has been ignored and the final protocol data has been used.

First, four bulbs are shown on *XY* axes with the same distance on a gridded screen, as shown in Fig. 2a. The bulbs that are labeled by 1, 2, 3 and 4 represent four main directions. In order to efficiently attract the subject's attention, the experiment begins on the screen with five seconds countdown that is shown in Fig. 2b. First, a bulb will be randomly switched on and remain on for 100 *ms* while the other three bulbs are off as depicted in Fig. 2c. When the first bulb switches off, the second bulb will be switched on after 150 *ms* and will remain on for the next 100 *ms*. This sequence repeats for all bulbs and after 1000 *ms*, the next round will start. To help the subjects to concentrate more, they are asked to select one bulb and count its flashes. For recognizing the selected bulb and consequently selected direction of the subject, this procedure will be repeated five epochs. A subject during the data recording is shown in Fig. 3 a. Left laptop displays test while the right one is connected to BCIs to record brain data.

2-2- Recording Device

Clinical EEG devices usually have 8, 16, 32, ... or 512 channels and an electrode is implemented to each channel. Typically, electrodes will be placed on the subject's head, which convey the critical potential to a preamplifier. Received signals will be amplified and filtered; then they can be recorded for further processing such as frequency spectrum analysis, classification, diagnostic algorithms and analog-to-digital conversion. In this project, the EEG device used to record data is Starstim made in Spain. This device can transfer data via eight channels. Transferred data is a $10 \times N$ matrix. First eight columns are the output of channels; the ninth column is the trigger and the last column is the simulation run-time.

The Neuroelecterics Instrument Controller (NIC) is a universal software solution that gives full control of Starstim device. NIC provides a user-friendly interface pack with a variety of features. One can manage recordings, launch recording sessions, stream data over the network and receive network triggers with NIC. This software is also able to send the data recorded by Starstim to MATLAB software by using TCP-IP protocol, simultaneously. Brain signals recording require some necessary prerequisites. By considering the brain's map that is shown in Fig. 4, primarily, the channels' locations should be specified. Then, the impedances should be checked in order to record the data with the highest quality.

2-3- Channel Selection

Different stimulated brain regions in different subjects, shown in Fig. 5, emphasize the necessity of a crucial channel selection. There are various methods for channel selection, depending on the environment and users conditions. Incomplete and improper selection causes difficulties in dimension reduction.

Here, certain bounds of channels in target and non-target signal categories are selected. Then, the correlation for the

Fig. 3: EEG signals recording.

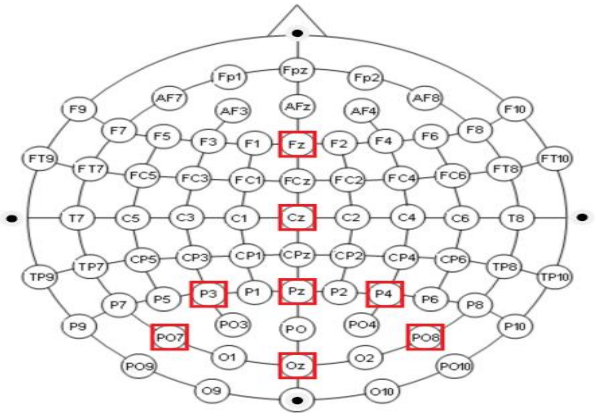

Fig. 4: The electrodes placement for eight channels.

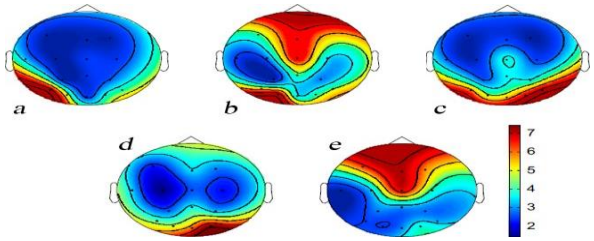

Fig. 5: Brain activity of five subjects during the test.

selected target signals is computed for all channels. Finally, channels with the lowest correlation are ignored [37]. Due to its high speed and accuracy, this method perfectly matches with real-time objectives. The final selected channels are $F_z, C_z, P_z, O_z, P_3, P_4, PO_7$ and PO_8.

3. Data Preprocessing

The next step after data recording is data processing. This step focuses on the quality and statistic assessment of the recorded signals and extraction of their content. In similar studies, the analysis of the training phase has a noticeable effect on the accuracy and efficiency of results. This effect emphasizes the importance of training and testing phase.

Band-Pass filtering is necessary to eliminate the noises of signals. However, to avoid a zero output and to prepare the signal for further preprocessing, offset trend, shown in Fig. 6a, should be removed. The signal with removed trends is also depicted in Fig. 6b. Then, the signal is filtered to eliminate all environmental noises, including blinking through a band-pass

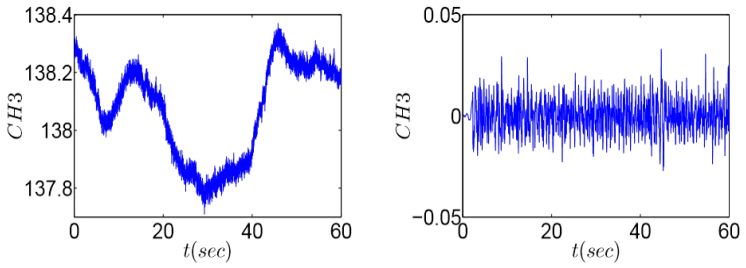

a b

Fig. 6: Recorded data from channel 3. a: The raw signal, b: Signal after removing trends.

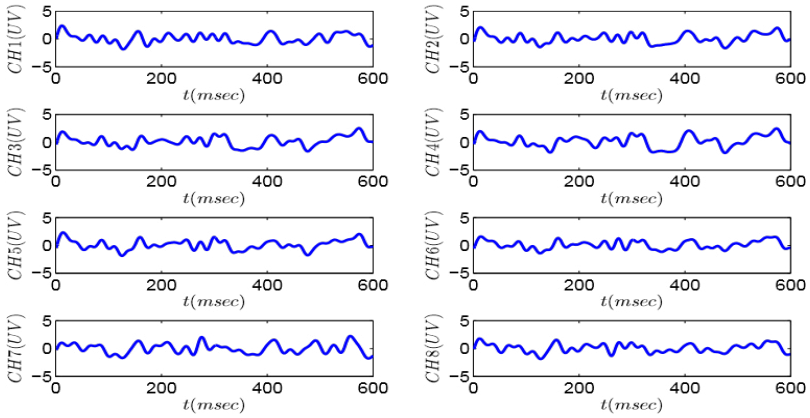

Fig. 7: The average of five consecutive epochs in range of 600 milliseconds for the first subject.

filter [30]. Sometimes, when the Electrooculography (EOG) and EEG signals amplitude surpass the threshold, there is no need to filter and the extracted parts must be excluded from the process. Because P300 components are observable at a frequency band between 1 to 15 HZ, the band-pass filter is designed to maintain these frequencies. After filtering, the signal is extracted to smaller parts based on the beginning of stimulation.

Increasing the accuracy and simplifying the computing are other advantages of using this frequency range. Afterward, the EEG signal is divided into epochs. Each epoch consists of 600 ms of EEG data after the stimulus onset. Every five successive epochs for each stimulus will be averaged to increase the SNR and enhance the accuracy of P300 detection. The output averaged epochs are shown in Fig. 7.

4. Feature extraction

Features usually reflect distinguishing characteristics, a noticeable measurement or a functional element obtained from data in hand. Extracted features are used to minimize and also simplify the number of resources needed to represent a large set of data accurately. Generally, the performance of a BCI system highly depends upon a suitable selection of both features and feature extraction techniques. Here, signal amplitude, Hilbert Huang and wavelet transform coefficients have been assigned as the features. Besides, principal component analysis (PCA) is used to reduce dimension of the feature space.

4-1- Hilbert Huang transform

Hilbert Huang transform (HHT) has been primarily developed for the analysis of the nonlinear and non-stationary signals. HHT is a way to decompose a signal into so-called intrinsic mode functions (IMF) along with a trend and to obtain the instantaneous frequency data [31]. IMF was introduced by Huang et al. [32] as the result of the Empirical Mode Decomposition (EMD). It is a necessary intermediate step toward computing instantaneous frequency through the Hilbert Transform or any other method. Technically, an IMF is a function that satisfies two conditions: (1) In the whole data set, the number of extrema and the number of zero crossings must be either equal or differ at most by one; and (2) At any point, the mean value of the envelope defined by the local maxima and the envelope defined by the local minima is zero [32]. These features guarantee a well-behaved Hilbert transform.

EMD method is used to decompose the signal into several IMF components. Then, the Hilbert Transform is applied to create an analytic signal and to obtain instantaneous frequencies and instantaneous amplitudes. So, the original features would be obtained.

The first IMF has the most similar frequency content and

it also has more zero-crossing points in comparison to the other functions. This fact makes the first function, the best alternative to calculate the instantaneous frequency of the input signal. In short, the instantaneous frequency calculation using the IMF is known as the Hilbert-Huang transform.

4-2- Wavelet transform

Among all time-frequency-transformations, wavelet is more operative on ERPs [33]. In ERP analysis, the signal phase must be considered and their frequency characteristics require processing in the time-frequency domain. The wavelet coefficients are used in $0-4$ *Hz* and $4-8$ *Hz* frequency bands that are named as Delta and Theta respectively. The quality of decomposition has a direct relation with the compatibility of signal and wavelet transform. In this study, the B-Spline wavelets are used because these types of wavelets are sub-optimal time-frequency localizer. They are also semi-orthogonal and have compact supports. These abilities make them quite prevalent.

4-3- Feature space reduction

Practically, only a small part of the features is essential and discriminative. Indeed, the feature space defined on the original signals may contain redundant information that does not have a significant influence on the features categorizing. Dimension reduction is applied to preserve more valuable information. Accordingly, the computation efforts drop and the system generalization capacity rises.

As a scale-invariant method [32], in this paper, PCA is applied for dimension reduction procedure. First, PCA sorts the eigenvalues of training covariance matrix from largest to smallest. Then, based on the problem definition, only information related to some of the largest eigenvalues are maintained. Finally, using their corresponding eigenvectors, the dimension of the secondary features space is reduced comparing to the primary one. Therefore, most of the initial features information will be kept in the secondary space. In Fig. 8, scatter plots for two components with the highest value in PCA are shown. These plots show how much one component is affected by another.

5. Classification

In BCI systems, classifiers are used to organize data based on their extracted features. There are so many methods which have been used for EEG signals classification. The k-nearest neighbors algorithm (k-NN) and support vector machine (SVM) are two classifiers which are used in this project.

5-1- Support vector machine (SVM)

In P300 BCI research, SVM is regarded as one of the most accurate classifiers [32]. A basic definition of SVM is provided in [35]. The main idea of a linear SVM is to find the separating hyperplane, between two classes such that the distances between the hyperplane and the closest points from both classes are maximal. In other words, we need to maximize the margin between the two classes. Although SVM is generally a two-class classifier, it can be developed

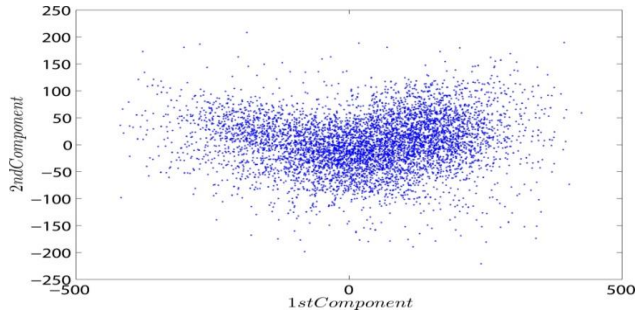

Fig. 8: Dimension reduction procedure.

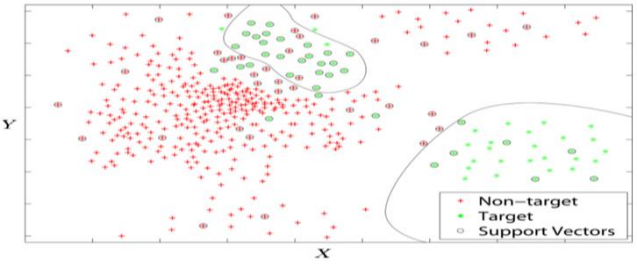

Fig. 9: Classification of learning data by SVM with optimized Gaussian center for the first subject.

for a multi-class application. Besides the linear classification, SVM can also perform a non-linear one by using kernel trick. Non-linear SVM can map their inputs into high-dimensional feature spaces. The two-dimensional feature space of training data set for the first subject is shown in Fig. 9. The target and non-target data are not utterly separable. Depending on the subject and the test, there are two or more target groups. As shown in Fig. 9, the targets are in two separate domains of the feature space. These two groups of targets have different characteristics, but they must be classified as one target group. This classification is indeed, independent of data distribution; therefore, realizing the training data distribution in the feature space is a necessary preliminary task.

Regardless of using some two-class or a multi-class SVM, a desirable performance is not always guaranteed. So, the k-NN algorithm, as an alternative solution and possibly better one is also tried.

5-2- The k-Nearest Neighbors Algorithm (k-NN)

k-NN is a training or supervision algorithm. Generally, this algorithm is utilized for two main purposes: (1) the distribution estimation of the training density function and (2) data classification according to the training template. The k-NN is used to classify the test data according to the training patterns. This algorithm is compatible with all types of data distribution. As shown in Fig. 9, our data are classified into two groups. These two groups are not entirely distinct in certain areas. Therefore, it is better to use a multi-class SVM. Mostly, selecting the two-class or multi-class character of the relevant samples related to the first category - which is the group in question- depends on the person or the decided exam. Indeed, using the multi-class SVM requires knowing

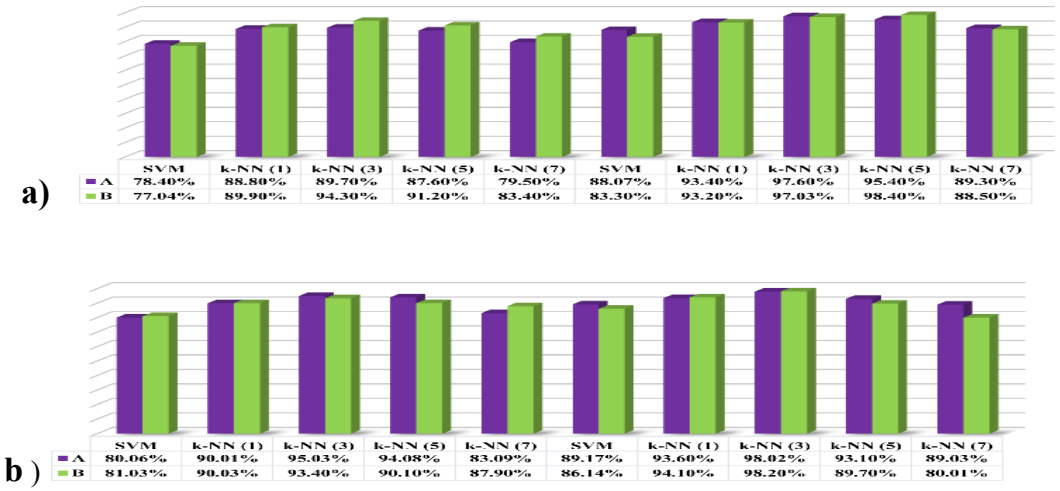

Fig. 10: Different classifier results for two groups of data sets; (a) BCI competition II, (b) recorded from subjects.

Table. 1: Statistical analysis . The experiments have shown that three neighboring has the best results in our project.

Classification Method	BCI Competition Data Base (subject A)	BCI Competition Data Base (subject B)	Subject 1	Subject 2
Based on Signal Domain (Averaged)	Ch = Cz : 38.8% Ch = Fz : 21.7% Ch = P3 : 8.08%	Ch = Cz : 27.6% Ch = Fz : 25.5% Ch = P3 : 7.8%	Ch = Cz : 37.6% Ch = Fz : 34.5% Ch = P3 : 12.3%	Ch = Cz : 41.5% Ch = Fz : 39.1% Ch = P3 : 17.5%
SVM with Optimized Center	88.07 % (32 channels)	83.3% (32 channels)	89.17 % (8 channels)	86.14% (8 channels)
K-NN	1-NN : 93.4% 3-NN : 97.6% 5-NN : 95.4% 7-NN : 89.3%	1-NN : 93.2% 3-NN : 97.03% 5-NN : 98.4% 7-NN : 88.5%	1-NN : 93.6% 3-NN : 98.02% 5-NN : 93.1% 7-NN : 89.03%	1-NN : 94.1% 3-NN : 98.2% 5-NN : 89.7% 7-NN : 80.01%

the methods of data distribution of the training features. On the other hand, applying KNN would eliminate this problem and is compatible with all distribution forms of traits.

Using one neighbor does not lead to suitable results and even may face errors, especially at the edge of the borders. Likewise, using five neighbors may cause the same errors. The experimental results show that using three neighbors is the best possible option for this project. The results for different classifiers considering two sets of data are compared in Fig. 10. The BCI competition II database, Berlin 2002, is used in Fig. 10a. Also, Fig. 10b is based on the recorded data of subjects.

As stated before, it is seen that if we utilize the one neighbor approach, we cannot achieve good results in the edges of the two groups and then we might face some errors. On the other hand, if we use five or more vicinities in certain areas, usually close to the edges, we might encounter some other difficulties. Our tests indicate that three neighbors will yield the best possible result. After comparing the results, you can see that the best results are of our database and has the nearest neighboring with the classifier in table.1.

The comparison results show that the best results come from our database by the k-NN classifier.

6. Robotic structure

Modeling and control of robotic arm have been paid tremendous attention in the field of mechatronics over the past few decades and the quest for a new development of robot arm control continues. Here, we are proposing some kind of cognitive robotic control.

In order to evaluate the proposed neuro-cognitive algorithm, the output of BCI is fed to a simulated 2-DoF robotic arm, shown in Fig. 11. The robot can move in a two-dimensional space (x-z plane) which provides an ability to do a variety of two-dimensional tasks including drawing shapes on a flat board, engraving on all kinds of surfaces or grabbing and moving any objects over a flat surface like playing chess or checkers. In this section, the dynamics and the control scheme of the robotic arm will be presented.

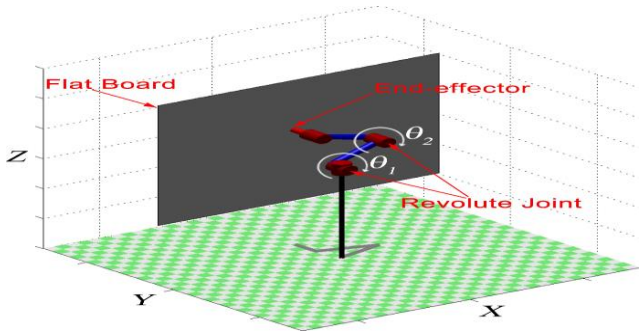

Fig. 11: A 2-DoF robotic arm.

6-1- Reference input

The output of the BCI module as the final subject decision is translated as a reference input to the robot control module. Indeed, by recognizing the subject's directional decision (up, down, left, or right), the robot will follow that movement correctly and consequently the control of the robot's end-effector would be realized. For example, if the initial position of robot's end-effector is (x, z) and the confirmed command from the BCI is detected as the up direction, the desired position (x_d, z_d) would be $(x, z + h)$ where h is the minimum resolution of the robot's movement. Similarly, for moving down, right and left, the desired position for the robot end-effector would set as $(x, z - h)$, $(x + h, z)$ and $(x - h, z)$, respectively. By this method, the subject will be able to control the position of the end-effector at each step in a real-time and point-to-point mode. In the next subsection, the dynamic of the robot would be presented.

6-2- Dynamics of the robotic arm

The target simulated robot is a robotic arm with two degrees of freedom. Dynamics of the proposed robotic structure is expressed by [36] as

$$M(\underline{\theta})\ddot{\underline{\theta}} + C(\underline{\theta}, \dot{\underline{\theta}})\dot{\underline{\theta}} + \underline{g}(\underline{\theta}) = \underline{u} \tag{1}$$

where $M(\underline{\theta})$ is the 2×2 inertia matrix of the manipulator. The index m_{ij} describes the effect of the acceleration of joint i on joint j. The inertia matrix is a symmetric positive definite matrix, whose indices are conFiguration dependent. C can be interpreted as the damping term in the model and $\underline{g}$ corresponds to the moment generated by the gravitational pull at each link and actuator. $\underline{\theta} = [\theta_1 \quad \theta_2]^T$ is the angular displacement of revolute joints and $\underline{u} = [u_1 \quad u_2]^T$ is the input torque vector to each joint.

6-3- Inverse dynamics control

This control algorithm is based on the exact linearization of all nonlinear dynamics of the system. It includes additional terms, actively providing the system with a spring-damper behavior. For tracking a given desired trajectory, (1) can be rewritten as:

$$M(\underline{\theta})\ddot{\underline{\theta}} + \underline{h}(\underline{\theta}, \dot{\underline{\theta}}) = \underline{u} \tag{2}$$

where $\underline{h}(\underline{\theta}, \dot{\underline{\theta}}) = C(\underline{\theta}, \dot{\underline{\theta}})\dot{\underline{\theta}} + \underline{g}(\underline{\theta})$. An inverse dynamics linearizing control signal $\underline{u}$ can be obtained as

$$\underline{u} = M(\underline{\theta})\underline{v} + \underline{h}(\underline{\theta}, \dot{\underline{\theta}}) \tag{3}$$

which will lead to the following system of double integrators

$$\ddot{\underline{\theta}} = \underline{v} \tag{4}$$

The new control signal $\underline{v}$ can now be chosen in such a way that the end-effector position, $\underline{x}$ follows the desired trajectory $\underline{x}_d$. This robotic arm has only two translational degrees of freedom as $\underline{p} = [x \quad y]^T$, i.e., the end-effector orientation is fixed. The end-effector's linear velocity is obtained by the help of Analytical Jacobian matrix as:

$$\dot{\underline{p}} = \begin{bmatrix} \frac{\partial x}{\partial \theta_1} & \frac{\partial x}{\partial \theta_2} \\ \frac{\partial y}{\partial \theta_1} & \frac{\partial y}{\partial \theta_2} \end{bmatrix} = J_A(\underline{\theta})\dot{\underline{\theta}} \tag{5}$$

Here $\underline{p} \in \mathbb{R}^2$ describes the position of the end-effector and $J_A(\underline{\theta})$ is the so-called Analytical Jacobian. Indeed, $J_A(\underline{\theta})$ corresponds to the mapping between the joint velocities and linear velocity of end-effector. By time differentiation of (5), the acceleration of end-effector can be expressed by:

$$\ddot{\underline{p}} = J_A(\underline{\theta})\ddot{\underline{\theta}} + \dot{J}_A(\underline{\theta}, \dot{\underline{\theta}})\dot{\underline{\theta}} \tag{6}$$

where $\dot{J}_A(\underline{\theta}, \dot{\underline{\theta}}) = \frac{\partial^2 \underline{p}}{\partial \underline{\theta}^2}\dot{\underline{\theta}}$. By the help of (4) and (6), a new control signal $\underline{v}$ can now be designed, in such a way that $\underline{p}$ tracks a given desired trajectory $\underline{p}_d$ as follows:

$$\underline{v} = J_A^{-1}(\underline{\theta})\left(\ddot{\underline{p}}_d + K_D\dot{\underline{e}} + K_P\underline{e} - \dot{J}_A(\underline{\theta}, \dot{\underline{\theta}})\dot{\underline{\theta}}\right) \tag{7}$$

In which K_P and K_D are positive definite diagonal matrices and $\underline{e} = \underline{p}_d - \underline{p}(\underline{\theta})$. Correspondingly, the error dynamics can be described by

$$\ddot{\underline{e}} + K_D\dot{\underline{e}} + K_P\underline{e} = 0 \tag{8}$$

The diagonal positive definite property of matrices K_P and K_D assures that the desired trajectory $\underline{p}_d$ would asymptotically be reached. By tuning the control parameters K_P and K_D, the different dynamic behavior of the system is acquired. The simulation model of the robot arm with implemented Inverse Dynamics Control is illustrated in Fig. 12.

7. Simulation

In this section, a simulation in MATLAB is given to evaluate the ability of BCI robotic structure. The task is to

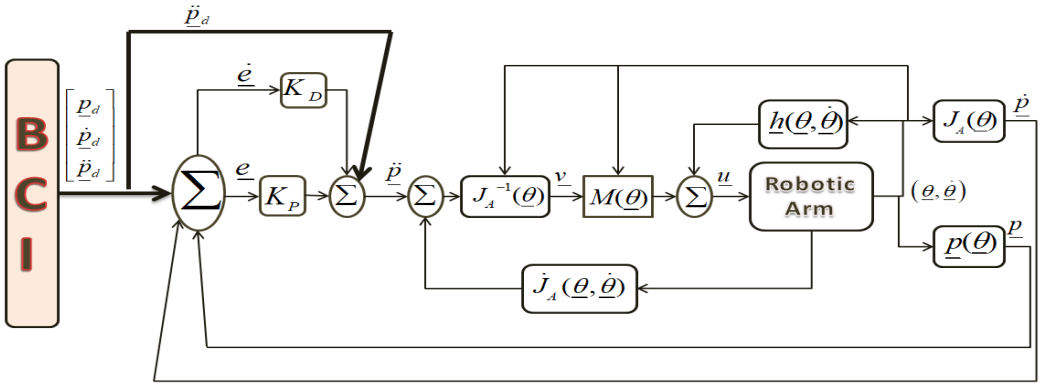

Fig. 12: Inverse dynamics control.

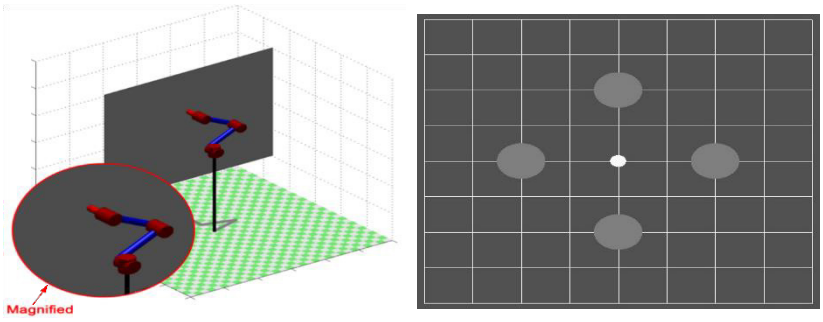

(a) (b)

Fig. 13: Initial state (a) Simulated robotic arm, (b) The BCI panel.

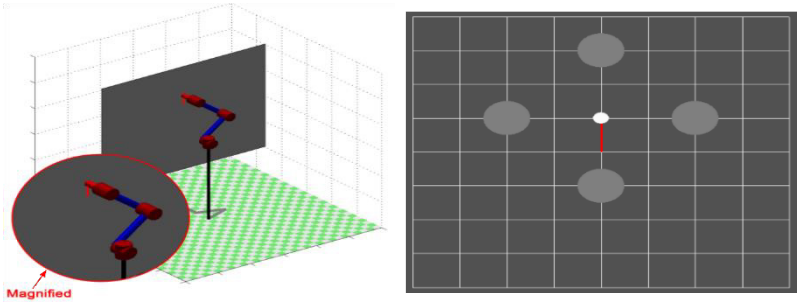

(a) (b)

Fig. 14: After the first detected decision (a) Simulated robotic arm, (b) The BCI panel.

draw some desired shapes on a vertical board via the BCI system which connects the user's brain to the 2-DoF robotic arm of Fig. 10. The robot's end-effector is attached to a marker for drawing. The subject imagines the desired shape in his mind and based on the required movements, at each step, focuses on the corresponding directions bulb in the BCI panel to move the tip of marker (attached to the end-effector). Indeed, BCI reads the confirmed direction, translate it for the robot controller as reference input and finally, the robot will draw the desired shape like a robotic hand.

As an example, drawing a letter like G is considered in details. The first step is to move the end-effector to the up direction. To achieve the first movement, the user must focus on the upper bulb. By that, the BCI system reads the brains signal, processes it, and sends the confirmed decision to the robot input unit.

This unit provides the desired reference input for the robot controller, corresponding to the robot fixed resolution. Then, the end-effector is moved in a way to reach the desired position by the control law. In Fig. 13, the initial position of the robot and BCI panel are shown. After receiving the first detected decision, the robot end-effector follows the controller inputs to meet the desired path, as shown in Fig. 14. In the next step of drawing letter G, the subject has to focus on the left flashing bulb. Then, by correspondingly focusing on the appropriate flashing bulbs in each step, letter G will be drawn on the board. Considering the counterclockwise handwriting, the sequence of subject concentrations is up-left-down-right-

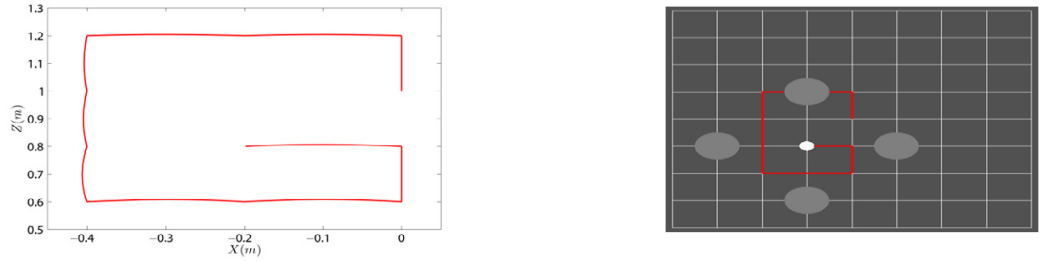

a) b)

Fig. 15: (a) Final robotic arm trajectory, (b) Final BCI panel display.

up-left. The resulting output of the BCI panel is shown in Fig. 15b. The output trajectory of the simulated robotic arm is also depicted in Fig. 15 a.

Regarding the data acquisition method, the drawn letter G is sharp-cornered and is not smooth. In this study, there were only four directions bulb, which finally lead to four distinct directions. Therefore, the robot movements are limited to these four directions, which cause hard corners in output shapes.

8. Conclusion

In this paper, recording methods, stimulus presentation paradigms, feature extraction, and classification algorithms of a P300 based BCI system were studied. We reached high accuracy in classification. The last stage of designing a BCI system is establishing a protocol for fast, accurate and efficient connection between brain, applications and external tools. In order to test the proposed algorithm, the BCI system was connected to a 2-DoF robotic arm. The overall structure comprises of BCI as the input and robot end-effector as the output. In this case, the user can control the robot's end-effector position by focusing on the desired direction's bulb. According to the mentioned applications of BCI systems, offline use of this type of systems is not functional and the main goal is being practiced in a real time application.

Further work and success of this research would lead to the development of robotic systems that can be deployed by disabled users, and thus improve their mobility, independence, and quality of life. In this regard, we are currently working on developing some robotic manipulators which are more compatible with BCI systems and improving the quality of attention detection based control schemes.

REFERENCES

[1] M. Higashima, K. Urata, Y. Kawasaki, Y. Maeda, N. Sakai, C. Mizukoshi, T. Nagasawa, T. Kamiya, N. Yamaguchi, and Y. Koshino, "P300 and the thought disorder factor extracted by factor-analytic procedures in schizophrenia," *Biological Psychiatry*, vol. 44, no. 2, pp. 115–120, 1998.

[2] J. Polich and K. L. Herbst, "P300 as a clinical assay: rationale, evaluation, and findings," *International Journal of Psychophysiology*, vol. 38, no. 1, pp. 3–19, 2000.

[3] R. Polikar, M. Greer, L. Udpa, and F. Keinert, "Multiresolution wavelet analysis of erps for the detection of Alzheimer's disease," vol. 3, pp. 1301–1304, 1997.

[4] A. R. Miller, C. Baratta, C. Wynveen, and J. P. Rosenfeld, "False memory: P300 amplitude, topography, and latency," *Running Head: P300 and False Recognition*.

[5] J. P. Rosenfeld, "Event-related potentials in the detection of deception, malingering, and false memories," in *Handbook of Polygraph Testing, M. Kleiner, Ed. New York: Academic Press*, 2002.

[6] L. A. Farwell and E. Donchin, "The truth will out: Interrogative polygraphy (lie detection) with event-related brain potentials," *Psychophysiology*, vol. 28, no. 5, pp. 531–547, 1991.

[7] J. B. Polikoff, H. T. Bunnell, and W. J. Borkowski Jr, "Toward a p300-based computer interface," in *RESNA95 Annual Conference and RESNAPRESS and Arlington Va*, 1995, pp. 178–180.

[8] L. Bi, X. A. Fan, and Y. Liu, "Eeg-based brain-controlled mobile robots: A survey," *IEEE Transactions on Human-Machine Systems*, vol. 43, no. 2, pp. 161–176, March 2013.

[9] M. A. Lebedev and M. A. Nicolelis, "Brain–machine interfaces: past, present and future," *TRENDS in Neurosciences*, vol. 29, no. 9, pp. 536–546, 2006.

[10] E. E. Thomson, R. Carra, and M. A. Nicolelis, "Perceiving invisible light through a somatosensory cortical prosthesis," *Nature Communications*, vol. 4, no. 1482, 2013.

[11] P. J. Ifft, S. Shokur, Z. Li, M. A. Lebedev, and M. A. Nicolelis, "A brain-machine interface enables bimanual arm movements in monkeys," *Science translational medicine*, vol. 5, no. 210, pp. 210 ra154–210ra154, 2013.

[12] J. Dethier, P. Nuyujukian, S. I. Ryu, K. V. Shenoy, and K. Boahen, "Design and validation of a real-time spiking-neural-network decoder for brain-machine interfaces," *Journal of neural engineering*, vol. 10 , no. 3, p. 036008, 2013.

[13] N. Birbaumer and L. Cohen, "Brain-computer interfaces: Communication and restoration of movement in paralysis," *PhysiologyLondon*, vol. 579, no. 3, pp. 621–636, 2007.

[14] N. Birbaumer, N. Ghanayim, T. Hinterberger, I. Iversen, B. Kotchoubey, A. Kubler, J. Perelmouter, E. Taub, and H. Flor, "A spelling device for the paralyzed," *Nature*, vol. 398, pp. R1–R13, 1999.

[15] L. J. P. M. H. L. Stopczynski A, Stahlhut C, "The smartphone brain scanner: A portable real-time neuroimaging system," *PLoS ONE*, vol. 9, no. 2, 2014.

[16] S.-S. Yoo, H. Kim, E. Filandrianos, S. J. Taghados, and S. Park, "Non-invasive brain-to-brain interface (bbi): establishing functional links between two brains," *PloS one*, vol. 8, no. 4, p. e60410, 2013.

[17] J. R. Wolpaw, D. J. McFarland, G. W. Neat, and C. A. Forneris, "An EEG-based brain-computer interface for cursor control," *Electroencephalogr. Clin. Neurophysiol.*, vol. 78, no. 3, pp. 252–259, 1991.

[18] Y. Li, C.Wang, H. Zhang, and C. Guan, "An EEG-based BCI system for 2d cursor control," in *Proc. IEEE Int. Joint Conf. Neural Netw.*, 2008.

[19] R. Krepki, B. Blankertz, G. Curio, and K. Muller, "The Berlin brain-computer interface (bbci): Towards a new communication channel for online control in gaming applications," *Computational and Mathematical Methods in Medicine*, vol. 33, no. 1, pp. 73–90, 2007.

[20] M. A. Nicolelis and M. A. Lebedev, "Principles of neural ensemble physiology underlying the operation of brain-machine interfaces," *Nature Reviews Neuroscience*, vol. 10, no. 7, pp. 530–540, 2009.

[21] A. J. Suminski, D. C., Tkach, A. H. Fagg, and N. G. Hatsopoulos, "Incorporating feedback from multiple sensory modalities enhances brain-machine interface control," *Journal of Neuroscience*, vol. 30, no. 50, pp. 16777–16787, 2010.

[22] D. Sussillo and L. F. Abbott, "Generating coherent patterns of activity from chaotic neural networks," *Neuron*, vol. 63, no. 4, pp. 544–557, 2009.

[23] A. H. Fagg, N. G. Hatsopoulos, V. de Lafuente, K. A. Moxon, S. Nemati, J. M. Rebesco, R. Romo, S. A. Solla, J. Reimer, D. Tkach *et al.*, "Biomimetic brain-machine interfaces for the control of movement," *Journal of Neuroscience*, vol. 27, no. 44, pp. 11842–11846, 2007.

[24] M. Thulasidas, C. Guan, and J. Wu, "Robust classification of EEG signal for brain-computer interface," *IEEE Transactions on Neural Systems and Rehabilitation Engineering*, vol. 14, no. 1, pp. 24–29, March 2006.

[25] E. M. Ventouras, P. Asvestas, I. Karanasiou, and G. K. Matsopoulos, "Classification of error-related negativity (ern) and positivity (pe) potentials using knn and support vector machines," *Computers in Biology and Medicine*, vol. 41, no. 2, pp. 98 – 109, 2011.

[26] A. Mahmoudi, S.Takerkart, F. Regragui, D. Boussaoud, and A. Brovelli, "Multivoxel pattern analysis for fMRI data: A review," *Computational and Mathematical Methods in Medicine*, 2012.

[27] E. Donchin, K. M. Spencer, and R. Wijesinghe, "The mental prosthesis: assessing the speed of a p300-based brain-computer interface," *IEEE Transactions on Rehabilitation Engineering*, vol. 8, no. 2, pp. 174–179, Jun 2000.

[28] Y. Li, H. Li, and C. Guan, "A self-training semi-supervised SVM algorithm and its application in an EEG-based brain-computer interface speller system," *Pattern Recognit. Lett*, vol. 29, no. 9, pp. 1285–1294, 2008.

[29] L. Wang, G. Xu, S. Yang, W. Yan, *et al.*, "Application of Hilbert-Huang transform for the study of motor imagery tasks," pp. 3848–3851, 2008.

[30] W. Pan, S. Ji-Zhong, and S. Jin-He, "Research of p300 feature extraction algorithm based on wavelet transform and fisher distance," *International Journal of Education and Management Engineering (IJEME)*, vol. 1, no. 6, p. 36, 2011.

[31] C. Cortes and V. Vapnik, "Support-vector networks," *Machine learning*, vol. 20, no. 3, pp. 273–297, 1995.

[32] N. E. Huang, Z. Shen, and S. R. Long, "The empirical mode decomposition and the Hilbert spectrum for nonlinear and non-stationary time series analysis," Proceedings of the Royal Society of London, A(454):903–995, 1998

[33] B. Siciliano, L. Sciavicco, L. Villani, and G. Oriolo, "Robotics modeling, planning and control," in *Advanced Textbooks in Control and Signal Processing*, 2008.

[34] H. K. Khalil, "Nonlinear systems," Prentice Hall, 2002.

[35] C. Cortes and V. Vapnik, "Support-vector networks," Machine learning, vol. 20, no. 3, pp. 273–297, 1995.

[36] B. Siciliano, L. Sciavicco, L. Villani, and G. Oriolo, "Robotics modeling, planning and control," in Advanced Textbooks in Control and Signal Processing, 2008.

[37] Yalda Shahriari and Abbas Erfanian, "ImprovingtheperformanceofP300-based brain–computer interface through subspace-based filtering", Neurocomputing 121, pp: 434-441, 2013

HOW TO CITE THIS ARTICLE

G. Garakani, H. Ghane, M.B. Menhaj, Control of a 2-DoF robotic arm using a P300-based brain-computer interface, AUT J. Model. Simul., 51(2) (2019) 153-162.

DOI: 10.22060/miscj.2019.15569.5136